Gold nanoparticles as absolute nano-thermometers.
Supporting information

Aquiles Carattino, Martín Caldarola, and Michel Orrit*

Huygens-Kamerlingh Onnes Lab, 2300RA Leiden, The Netherlands

E-mail: orrit@physics.leidenuniv.nl

Anti-Stokes emission form gold nanorods

We model the photoluminescence generation in gold nanorods with successive steps taking place between absorption of light and re-emission of luminescence.[1] Figure S1 shows the energy-momentum representation of the photoluminescence processes in gold nanorods. After excitation with monocrhomatic light of energy $\hbar\omega_L$, a collective oscillation of electrons is generated, i.e. a surface plasmon (SPR). Once the plasmon coherence is lost (dephasing time $\sim$fs), the state can be described as an electron-hole pair. Then, different scenarios are possible: recombination without energy exchange, elastic recombination (leading to Rayleigh scattering) or recombination with energy exchange. In this case, three scenarios are possible: electron and hole may recombine radiatively after one or more interactions with the thermal baths of lattice phonons and charge carrier thermal excitations: i) if the energy difference between electron and hole states is lower than the initial one after excitation we obtain Stokes emission upon a radiative recombination; ii) if electron and hole transiently increase their energy difference at the bath's expense before recombining radiatively, we observe anti-

1

Stokes emission; iii) if electron and hole recombine non radiatively, their energy difference is transferred to the baths and no photon is emitted. The latter process is the most probable one, explaining the low yield of luminescence in gold ($\sim 10^{-6}$).
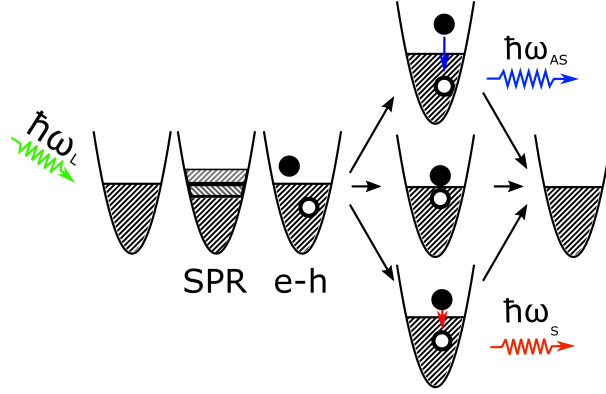

Figure S1: **Schematic representation of Stokes and Anti-Stokes luminescence process from a single gold nanorod.** Upon the excitation with resonant energy $\hbar\omega L$ a surface plasmon is created (SPR), which creates an electron-hole pair state (e-h). This pair can recombine non-radiatively (the most likely event) or radiatively after iterating with the baths, leading to high energy (anti-Stokes) or low energy (Stokes) emission of a photon.

Experimental setup

The experimental setup consisted on a home-made confocal microscope, schematically shown in figure S2, similar to the one presented before.[1] The microscope allows the detection of individual nanorods in the sample and the measurement of their photoluminescence spectra. We use continuous wave lasers at 532 nm or 633 nm to excite the transverse and longitudinal plasmon resonances, respectively. The 532 nm is a DPSS laser (CNI) and the 633 nm is a HeNe (Thorlabs). Both lasers are reflected at a 50/50 beam splitter that allows the simultaneous detection of the anti-Stokes and Stokes emission of the particles.

We employ an objective lens to focus the excitation beam into a diffraction-limited spot and we collect the emitted photoluminescence using the same objective in an epi-configuration. The 532 nm laser is focused down by our 60x NA1.4 objective to a waist of 228 nm, with a power of 200μW reaching the sample, leading to an intensity of 1.23

mWμm^{-2}. For the HeNe laser, the maximum power used was 100 μW which corresponds to 0.43 mWμm^{-2}. This is equivalent to 1.37×10^{15} photons s^{-1} μm^{-2}, which leads to a fluence of ≈ 240 photonsμm^{-2} in three minutes integration time used for the spectra acquisition. A confocal pinhole of 50 μm is placed between a pair of lenses with 10 cm focal length to reduce the unwanted background from the solvent above the nanorods. Then we could select between an APD or the spectrometer to perform a raster-scan image or an emission spectrum, respectively. We reject the laser light with appropriate notch filters.

Additionally, the temperature of the sample can be controlled with a special holder that allows water flow, a heater and a thermocouple to measure the temperature of the sample. For the experiments done with this holder we employed a 60X objective with NA 0.9 (Olympus) to avoid presence of a heat sink on the particle under study.

Gold nanorods sample characterization

We synthesized gold nanorods using the seed-mediated growth method[2] and characterized their size by performing TEM imaging on a drop-cast sample on a silicon substrate. Figure S3 (a) shows the image where the cylindrical shape with spherical caps can be seen and the width is 23 nm while the length is 50 nm, leading to a mean aspect ratio of 2.17. Naturally, there is some size dispersion due to the fabrication procedure, that leads to a broad bulk extinction spectra, shown in (b). The transverse plasmon resonance is located at 525 nm while the more intense longitudinal plasmon resonance is at 630 nm. We also show the wavelengths of the lasers used for our study as vertical lines.

Determination of the error in the temperature extraction

The phenomenological model we use to extract the temperature from the anti-Stokes spectrum depends on the prior determination of shape and position of the surface plasmon resonance (SPR). In our case, we measure the photoluminescence emission spectrum when
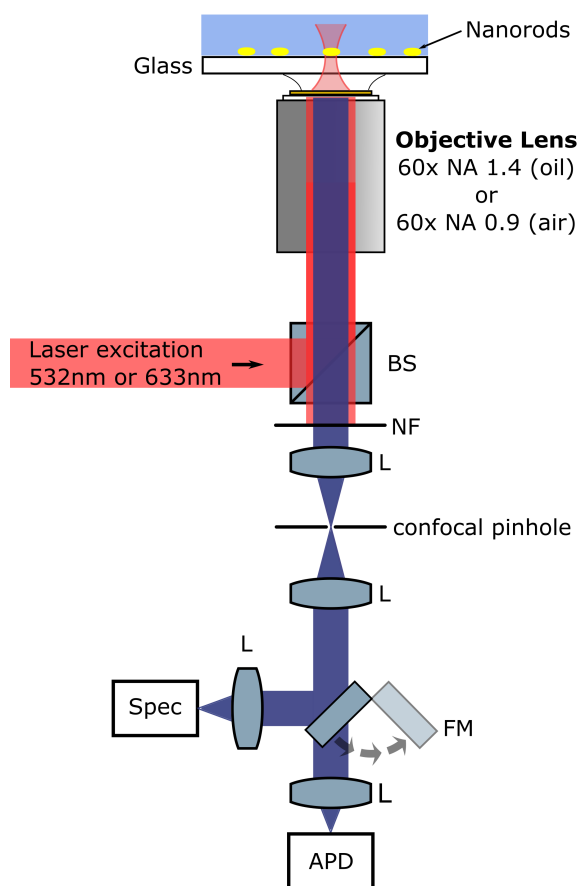
Figure S2: **Scheme of the experimental setup.** The sample consists of individual gold nanorods immobilized on glass. BS: beam splitter. NF: notch filter to remove excitation light and detect Stokes and anti-Stokes photoluminescence. L: lens. FM: flip mirror. SPEC: spectrometer. APD: avalanche photodiode.
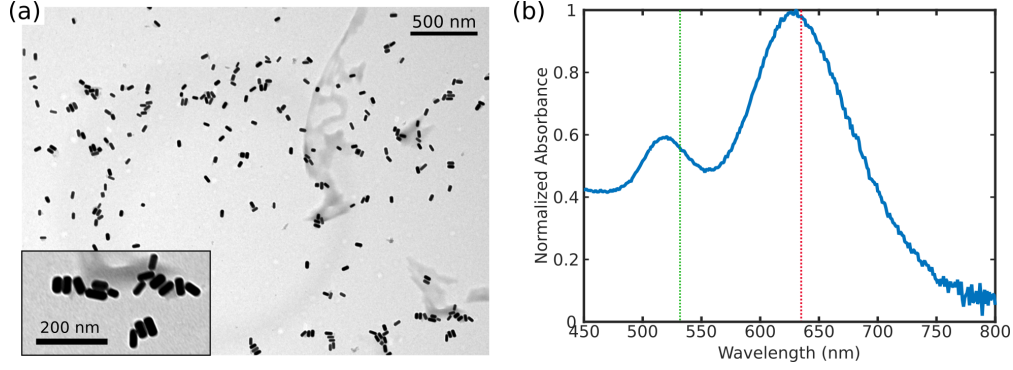
Figure S3: **Gold nanorod characterization.** (a) TEM image of a dried drop of the gold nanorods used in this study. The mean width is 23 nm while the length is 50. The inset shows higher magnification. (b) Bulk absorbance spectra of the gold nanorod sample showing the transverse (around 525 nm) and the longitudinal (around 630 nm) surface plasmon resonances. The dashed vertical lines show the two laser wavelengths used in this work.

a single nanorod is excited with a 532 nm CW laser. Figure 1 in the main text shows an example of such spectra for an individual nanorod. An asymmetric shape is measured, due to a broadband contribution from gold added to the plasmonic emission. This leads to a complication to determine the SPR since a simple Lorentzian shape does not fit this data. We present in the following two ways to circumvent this problem that lead to similar quantitative results.

The first one consist on determining the background phenomenologically with independent experiments and take it into account for the SPR determination. The second one consists on fitting a portion of the photoluminescence spectra to a Lorentzian to extract the correct SPR. In both cases we analyze the errors and compare the results, obtaining quantitatively equivalent results.

Background subtraction

In this case we modeled this emission spectra taken with the 532 nm laser with the following phenomenological form

$$I_{\mathrm{PL}}(E) = A_1 B(E; \Delta) + A_2 I_{\mathrm{SPR}}(E) , \tag{1}$$

where E represents the photon energy, B is the broadband contribution from bulk gold, phenomenologically modeled as $B(E; \Delta) = \exp(E/\Delta)$, $I_{\mathrm{SPR}}(E)$ surface plasmon resonance spectra and A_1 and A_2 are constants. We take the SPR to be Lorentzian,[3] i.e.

$$I_{\mathrm{SPR}}(E) = \frac{(\Gamma/2)^2}{(E - E_{\mathrm{SPR}})^2 + (\Gamma/2)^2}. \tag{2}$$

Figure S4(a) presents some individual gold nanorods spectra with size similar to the ones presented in the main text, i.e. a bulk SPR around 635 nm. We use this set of spectra to empiricaly obtain the shape of the background. Figure S4(b) shows an example of the fitted function and the extracted function $B(E; \Delta)$. We performed this fit on five different nanorods and we averaged the values for Δ, obtaining $\Delta = (0.120 \pm 0.02)$ eV. We then fix this parameter, which defines our background model and analyze an independent set of data from a single nanorod to retrieve the temperature with the procedure we present in this paper.
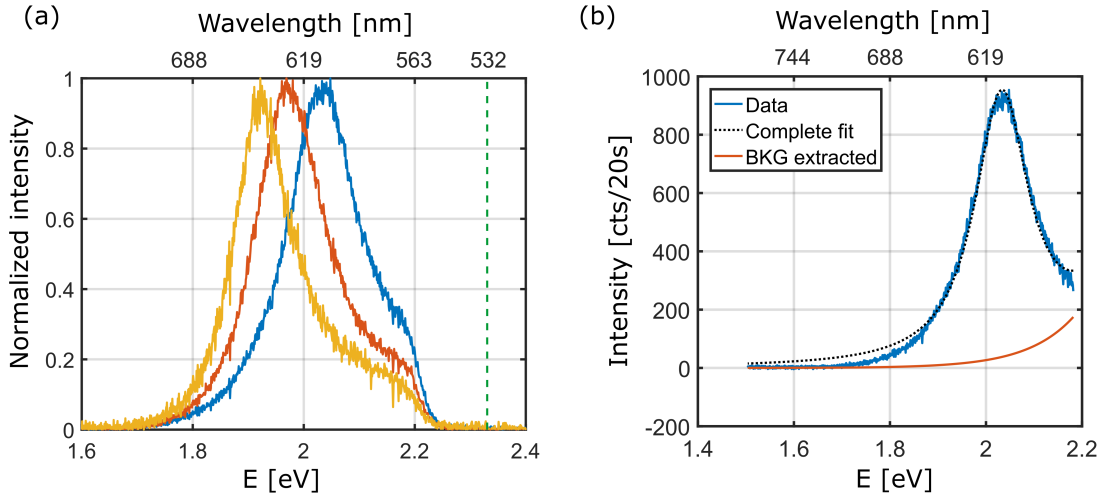

Figure S4: **Photoluminescence spectra of individual gold nanorods.** (a) Normalized emission spectra of three different individual nanorods, all of which present an asymmetric shape due to the bulk emission contribution. The vertical dash line shows the excitation laser energy and the abrupt cut close to 2.2eV is due to the notch filter used to prevent laser detection.(b) Example of the fit to extract the function $B(E; \Delta)$. The blue solid line is the spectra of an individual nanorod and the black dotted line is the fitted function from 1. The red solid line shows the obtained function $B(E; \Delta)$. The integration time in the spectra acquisition for these spectra was 20 s.

The first step in our protocol is to find $I_{\text{SPR}}(E)$. We did that by fitting photoluminescence spectra recorded with 532 nmlaser excitation of the nanorod under study with the function 1 with Δ as a fixed taken from our previous analysis. The inset in figure S5 (a) shows the spectra and the fit, which provides the parameters that characterize the SPR, i.e. SPR (E_{SPR}, Γ). Then we fit the anti-Stokes part of the spectra obtained with nearly resonant excitation of 633 nm, obtaining the curves shown in figure S5 (a). With the obtained temperature values for each laser power we construct the plot in figure S5 (b), where the error bars correspond to the square root of the variance of the temperature, estimated by the fitting algorithm. Note that the higher the power, the smaller the error, due to the higher photon counts in the spectra. We emphasize that a single spectra leads to a temperature value with a relative error of 2% for powers larger than 70 mW.

Additionally, we performed a linear fit to these temperature values and extrapolated to zero laser power, which corresponds to room temperature. We obtained a value of $T_r = (297 \pm 13)$ K, consistent with independent measurements and a 4% relative accuracy.

Fit a Lorentzian in a restricted range

In this case we model the emission with 532 nm excitation with a simple Lorentzian (see equation 2), but we take a minimum wavelength for the fitting. This avoids the contribution of the background, which is significantly higher at the low-wavelength part of the spectra. Due to the presence of this cut, the fitting of the SPR function of equation is not univocally determined; it will depend on the cut wavelength λ_c used for the fit. Therefore, we need to evaluate the error that such a procedure introduces for the temperature extraction.

Luminescence power dependence

Figure S6 shows the intensity of the Stokes (red) and anti-Stokes (blue) emission for several excitation powers. In both cases the linear fit in logarithmic scale has a slope close to 1,
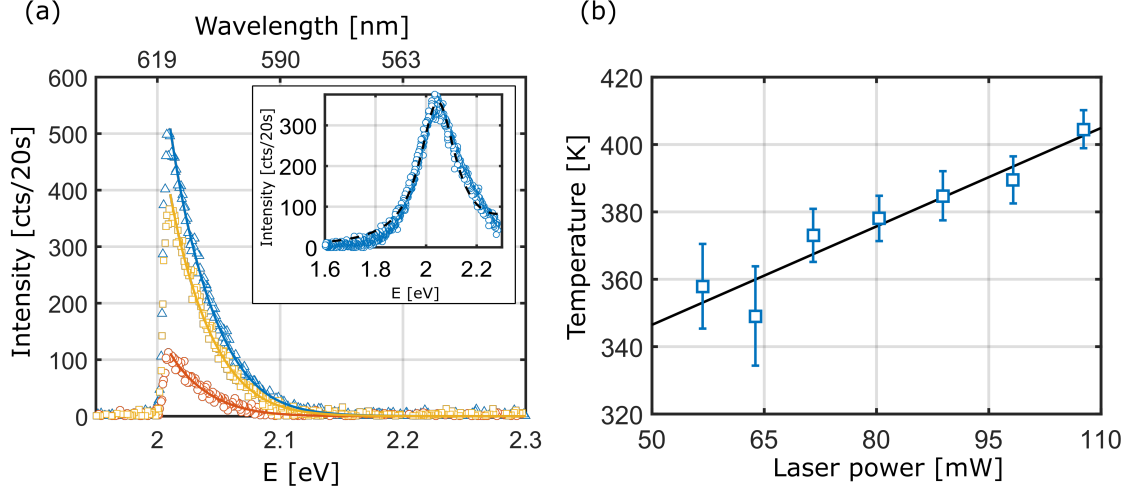
Figure S5: **Temperature extraction from the anti-Stokes emission.** (a) Anti-Stokes spectra for three different 633 nm-excitation power: 107 mW in blue triangles, 88 mW in yellow squares and 63 mW in red circles. The solid lines correspond to the fit using our model from equation 2 in the main text, with T as a free parameter. The inset shows the photoluminescence spectra of the same nanorod excited with 532 nm (blue circles) and the fit using the equation 1 with a fixed value for Δ (dashed black line), from which we obtained $E_{\mathrm{SPR}} = 2.04$ eV and $\Gamma = 0.175$ eV. (b) Temperature extracted from the spectra in (a) for different laser excitation power. The solid black line corresponds to a linear fit that gives a room temperature value $T_r = (297 \pm 13)$ K.
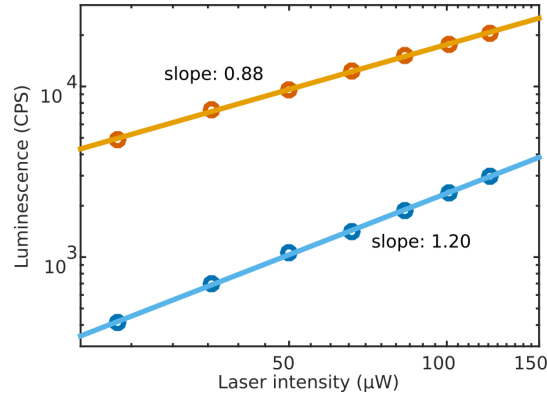

Figure S6: **Stokes and anti-Stokes integrated emission as a function of excitation power.** The linear fit in logarithmic scale has a slope of 0.88 and 1.20 respectively, confirming the 1-photon nature of both kinds of emission.

being 0.88 for the Stokes and 1.20 for the anti-Stokes, confirming that both types of emission are single-photon processes. The anti-Stokes band has a higher slope due to dependence on T of the anti-Stokes emission and to nanorod heating at higher power: the higher the power, the higher the temperature of the particle and the higher the anti-Stokes signal is. This behavior is independent of the plasmon resonance position. It is important to note that the excitation intensity cannot be increased much beyond what is shown because nanorods would start reshaping towards more spherical shapes at higher laser powers.
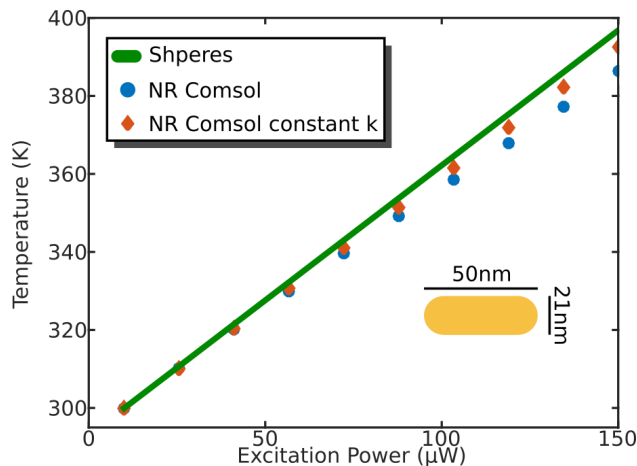
Gold Nanorod temperature numerical calculations

Figure S7: **Gold nanorod temperature calculation for different excitation powers.** Calculated temperature for a nanosphere (full line) and for a 21 nm × 50 nm nanorod (dots) under different excitation intensities. The dots are numerically calculated values using COMSOL Multiphysics commercial software. The blue dots where obtained with the temperature-dependent heat conductivity of water and the red diamonds with a constant value of $0.61\,\mathrm{W(m\cdot K)}^{-1}$.

Throughout the main text the temperature measured with the anti-Stokes emission is compared to the calculated temperature using the heat diffusion equation. For spheres in an homogeneous water environment and assuming an infinite thermal conductivity for the metal, the temperature increase is given by

$$\Delta\mathrm{T}(P) = \frac{P}{4\pi k_{\text{water}} R} \tag{3}$$

where P is the dissipated power, k_{water} is the heat conductivity of water and R is the radius of the particle.[4] The dissipated power can be easily derived from the cross section of the particle at a given wavelength and the intensity of the focused laser beam. For nanorods we assumed an equivalent sphere with radius such that the total rod area is preserved.

Figure S7 shows the difference between the results from the sphere (full line) and a finite element method calculation (dots) for a nanorod of length 50 nm and diameter 21 nm. The cross section and dissipated power were kept the same. The blue dots are the results given by using the built-in material properties of water, i.e. a thermal conductivity that depends on temperature. The red diamonds are the results when the thermal conductivity is fixed to $0.61 \, \mathrm{W(m \cdot K)^{-1}}$. The difference is accentuated at higher temperatures.

References

(1) Carattino, A.; Keizer, V. I.; Schaaf, M. J.; Orrit, M. Background suppression in imaging gold nanorods through detection of anti-stokes emission. *Biophysical journal* **2016**, *111*, 2492–2499.

(2) Nikoobakht, B.; El-Sayed, M. A. Preparation and growth mechanism of gold nanorods (NRs) using seed-mediated growth method. *Chem. Mater* **2003**, *15*, 1957–1962.

(3) Zijlstra, P.; Orrit, M. Single metal nanoparticles: optical detection, spectroscopy and applications. *Reports Prog. Phys.* **2011**, *74*, 106401.

(4) Baffou, G.; Quidant, R. Thermo-plasmonics: using metallic nanostructures as nano-sources of heat. *Laser Photon. Rev.* **2013**, *7*, 171–187.